The Application of Raman and anti-Stokes Raman Spectroscopy for In-situ Monitoring of Structural Changes in Laser Irradiated Titanium Dioxide Materials.

Stephanie J. Rigby[1], Ala H.R. Al-Obaidi [2], Soo-Keun Lee[3], Daniel McStay[4] and Peter K. J. Robertson[1*]

[1] Centre for Research in Energy & Environment, School of Engineering, The Robert Gordon University, Aberdeen AB10 1FR, United Kingdom.

[2] Smart Light Devices, Unit 13, Tyseal Base, Craigshaw Crescent Aberdeen, West Tullos Industrial Estate, Aberdeen, AB12 3AW, United Kingdom.

[3] School of Environmental Science and Engineering, POSTECH, San 31 Hyoja Dong Nam-Gu, Pohang, Kyungpook, 790-784, Korea

[4] Discovery Technologies Ltd, Redshank House, Alness Point Business Park, Alness, IV17 0IJ, UK.

* Corresponding author: Tel: +44 1224 262301, Fax: +44 1224 262222.

E-mail address: peter.robertson@rgu.ac.uk

Keywords: TiO_2, photocatalyst, Raman spectroscopy, laser irradiation.

Abstract.

The use of Raman and anti stokes Raman spectroscopy to investigate the effect of exposure to high power laser radiation on the crystalline phases of TiO_2 has been investigated. Measurement of the changes, over several time integrals, in the Raman and anti-stokes Raman of TiO_2 spectra with exposure to laser radiation is reported. Raman and anti-stokes Raman provide detail on both the structure and the kinetic process of changes in crystalline phases in the titania material. The effect of laser exposure resulted in the generation of increasing amounts of the rutile crystalline phase from the anatase crystalline phase during exposure. The Raman spectra displayed bands at 144 (A1g), 197 (Eg), 398 (B1g), 515 (A1g), and 640 (Eg) cm^{-1} assigned to anatase which were replaced by bands at 143 (B1g), 235 (2 phonon process), 448 (Eg) and 612 (A1g) cm^{-1} which were assigned to rutile. This indicated that laser irradiation of TiO_2 changes the crystalline phase from anatase to rutile. Raman and anti-stokes Raman are highly sensitive to the crystalline forms of TiO_2 and allow characterisation of the effect of laser irradiation upon TiO_2. This technique would also be applicable as an *in-situ* method for monitoring changes during the laser irradiation process.

1. Introduction

The use of titanium dioxide (TiO_2) as a photocatalyst for the degradation of chemical and biological species in the environment has generated a significant level of scientific interest over the past 20 years [1-4]. This material has also been used in novel solar cells where TiO_2 acts as a dye-sensitised photo-anode [5,6]. The photo-catalytic activity of TiO_2 is dependent upon a number of factors including, surface area, annealing temperature, crystalline structure light intensity and substrate adsorption and concentration [1-6]. Consequently unless all these factors are similar for different materials it may be difficult to compare the photocatalytic activity of different TiO_2 photocatalyst materials. Thus the results of work performed in one laboratory may not always be compared with that of another. Frequently, however, the effectiveness of photocatalysts are compared in terms of the rates of pollutant destruction over a particular time period together with the photonic efficiencies for these processes. The two most important photo-active forms of TiO_2 are anatase and rutile, though in many photocatalytic reactions anatase has been reported to shows a higher activity than rutile [7]. This increased performance in photo-activity has been explained by the fact that the Fermi level of anatase is higher than that of rutile by 0.1 eV [2]. Interestingly, however, one of the most photocatalytically active TiO_2 materials, Degussa P25, contains a small amount of rutile in the predominantly anatase structure (approximately 25% rutile to 75% anatase) [4]. This enhancement in photo-activity cannot be explained by individual activity of each crystalline phase but is probably related to the creation of complex structures (for example capped or coupled type heterostructures) of rutile and anatase [2]. One problem with the argument that rutile is less photocatalytically active than anatase is the fact that when anatase material is converted to rutile by sintering above 600 ^{o}C, not only is the

crystal structure changed, but the particle size and surface area are changed. It is therefore possible that the reduction in photocatalytic activity may be due to the reduction in surface area rather than the change in crystal structure.

TiO_2 is known to exist in three crystalline phases rutile, anatase (both tetragonal) and brookite (orthorhombic) [1-3]. The anatase and rutile phases have the same fundamental structural unit but different modes of arrangement and links. Each crystalline form belongs to a different space group [1-3]. The rutile structure has a space group D_{4h}^{14} and lattice constants a = 0.4954 and c = 0.2958 nm, while anatase belongs to the space group D_{4h}^{19} and has lattice constants a = 0.3783 and c = 0.951 nm. Brookite has a rather different space group - D_{2h}^{15} and lattice constants a = 0.9184, b = 0.5447 and c = 0.5145 nm.

Raman spectroscopy is a very effective means of detecting these different crystalline phases in TiO_2 powders and the assignment of observed bands to rutile, anatase and brookite has been reported [8-14]. These crystalline phases are not thermodynamically stable as both anatase and brookite transform irreversibly and exothermically to rutile when heated to high temperatures [10,15,16]. We have previously reported that, when irradiated with laser light the crystal phase of anatase TiO_2 transforms to rutile with the simultaneous generation of Ti(III) sites in the material [17-19]. The particle size and surface area or the laser treated materials however were unchanged. Interestingly the photocatalytic activity of this material was unaltered following treatment. To date there have been no reports of the use of Raman spectroscopy to monitor the effect of intense laser irradiation upon the crystalline phases of TiO_2. This technique would be particularly useful as a method where the

changes could be monitored *in situ* while the materials were be subjected to the laser treatment. In this paper we report some the application of Raman and anti-Stokes Raman Spectroscopy to monitor laser induced effects on Degussa P25 TiO_2 powders.

2. Experimental

TiO_2 (Degussa P25) was used as supplied. The laser source for irradiation of the TiO_2 was a Continuum Surlite tripled Nd:YAG laser operating at 355 nm. This produced 4.5 ns pulses of 10 MW peak pulse power. Irradiation of the samples was carried out by placing 20 mg of TiO_2 directly in the laser beam for varying times. The TiO_2 powder was shaken every two minutes during laser radiation. Heating of the samples, where applicable, were performed in an oven set at 450 ^oC.

Raman spectroscopy measurements were recorded using an Argon ion laser operating at 514 nm. The laser power directed at the sample was measured to be 500 mW. The laser line was filtered to remove any traces of plasma lines using a 1 nm interference filter centred at 514 nm. A silver spot mirror with 3 mm diameter was used to direct the laser beam onto the sample. The laser spot size at the sample is about 25 μm in diameter which was imaged at the slit (slit width 10 μm) of the spectrograph (Oriel 260i spectrograph) using a 180^o-back scattering geometry as shown in Fig. 1. The Raman signal was filtered before passing through the spectrograph using a notch filter. The Raman signal was detected using a water cooled front illuminated CCD detector (Oriel model DU401) cooled to -80^o C and analysed using a PC. A schematic representation of the experimental set-up is given in Fig. 1.

.

3. Results and Discussion

Raman spectra of the three crystalline phases of TiO_2 have been well reported [8-14]. Rutile has four Raman active modes $A_{1g} + B_{1g} + B_{2g} + E_g$ [15], anatase has six Raman active modes $A_{1g} + 2B_{1g} + 3E_g$ [15] and Brookite has 36 Raman active modes [20]. The Raman stokes spectrum of TiO_2 before and after laser irradiation treatment for 10 min is shown in Fig. 2. Fig. 2(a) shows the Raman spectra of the untreated TiO_2. These Raman bands are assigned to a mixture of anatase and rutile forms of the TiO_2. Strong Raman bands at 144 (E_g), 398 (B_{1g}), 515 (A_{1g} , B_{1g}), and 640 cm^{-1} (E_g) were observed along with a weak band at 197 cm^{-1} (E_g) which were assigned to the anatase form of TiO_2 in accordance with the literature [8-14]. This data is summarised in Table 1. The intensity of the band at 144 cm^{-1} was reduced by interference from the notch filter. Weak Raman bands at 235 (combination), 448 (E_g) and 612 cm^{-1} (A_{1g}) were also observed in Fig. 2(a) and were assigned to the rutile form of TiO_2. Thus, the TiO_2 sample before irradiation had Raman bands dominated by the anatase form with some of the rutile form also present.

Following irradiation for 10 minutes with the laser at 355 nm, the TiO_2 sample produced a distinctive Raman spectrum as shown in Fig. 2(b). It can be seen that new Raman bands at 146, 236 and 1050 cm^{-1} were observed, along with Raman bands at 448 and 612 cm^{-1} which were present in much greater intensity than in the original sample (Fig. 2(a)). Mathematical subtraction of the starting spectrum from the spectrum of the irradiated TiO_2 produced a spectrum (Fig. 2(c)) entirely due to the newly created species. This spectrum had strong bands centred at 236, 448 and 612 cm^{-1} along with a weak band at 146 cm^{-1}. It has been reported that the rutile form of TiO_2 exhibits Raman bands at 235, 447 and 612 cm^{-1}. Therefore, the spectrum in Fig.

2(c) was assigned to the rutile form of TiO_2. These results thus indicate that the anatase form of the TiO_2 was converted to rutile form during laser irradiation. Further complex(es), however, may also have been generated since a band at 146 cm^{-1} and a very broad band centred at 1050 cm^{-1} were also present (Fig. 2(c)). These bands are not reported to originate from the rutile or the anatase forms of TiO_2 and further studies are required to assign these bands.

Anti-Stokes Raman spectra of TiO_2 following exposure to 355 nm were also recorded (Fig. 3). The spectra showed bands centred in the same positions as found with the Raman spectra in Figure 2. The relative intensities of the vibrational bands for the starting material recorded with anti-stokes Raman were different to the corresponding Raman spectra. The band centred at 398 cm^{-1} had the highest relative intensity in the anti-Stokes Raman spectra (Fig. 3a) in contrast to the Raman spectra (Fig. 2a) which showed a band centred at 640 cm^{-1} having the highest relative intensity (excluding the E_g band at 144 cm^{-1}). The effect of laser exposure upon TiO_2 produced an increase in intensity of bands at 448 and 612 cm^{-1} while the bands at 398, 515 and 640 cm^{-1} decreased in intensity. The bands were in the same position as observed in the Raman spectrum (Fig. 2b). Therefore the assignment of these spectra indicated that that anatase was converted to rutile. Mathematical subtraction of the starting materials spectrum from the spectrum of the irradiated TiO_2 produced a spectrum (Fig. 3c) that had bands centred at 448, and 612 cm^{-1}. The E_g band at 398 cm^{-1} (Fig 3a) was the most intense band observed in the anti-stokes spectra of TiO_2. Laser irradiation of the sample reduced the intensity of this band, while shifting its position to 448 cm^{-1} (Fig 3b). The spectral features were the same as found with the Raman spectra shown in Fig 3, where the relative intensities, band positions and band widths of these two

bands were approximately equal for both the anti-stokes Raman spectrum (Fig. 3c) and for the Raman spectrum (Fig. 2c). This further confirmed that anatase material was converted to rutile.

In order to study the kinetics of the conversion of the anatase to rutile phases, the Stokes and anti-Stokes Raman spectra were recorded at several time integrals (Figs. 4 and 5). An increase in the intensity of the bands associated with the rutile form and a decrease in the intensity of the anatase form were observed with laser irradiation time. The data shown in Fig. 4 was further analysed by plotting the rise and fall of the bands at 236 and 515 cm^{-1}, which are associated with the rutile and anatase forms, (Fig. 6 and Table 1.) This clearly showed the kinetics of the conversion of the anatase to rutile as a function of time.

Further investigations of the effect of laser irradiation upon TiO_2 were undertaken by investigating the effect of heat on TiO_2 following laser irradiation. The effect of subsequent heating of the TiO_2 was found to depend upon the sample irradiation time prior to the thermal treatment. A TiO_2 sample irradiated for two minutes (Fig. 7a) and a sample irradiated for 10 minutes (Fig. 7c) were found to produce different amounts of rutile crystal phase when subjected to a subsequent heat treatment in a furnace for the same time. This was observed through examination of the intensity of bands associated with the rutile phase (240, 448 and 612 cm^{-1}) compared to bands assigned to the anatase phase (398, 515 and 640 cm^{-1}). The TiO_2 sample irradiated for two minutes (Fig. 7a) was found to be a mixture of predominantly anatase with some rutile also present. Following heating in furnace (Fig. 7b) the rutile phase increased in intensity to a degree comparable to the spectrum shown in Fig 4c, which was the

spectrum of TiO_2 irradiated for four minutes. For the TiO_2 sample irradiated for 10 minutes followed by heating (Fig 7d) the rutile phase was further generated at the expense of the anatase phase, with the rutile phase predominating. An examination of Fig. 7d showed that only one band from the anatase phase (the band at 515 cm^{-1}) was clearly visible. This band had a very low intensity compared to the other bands centred at 236, 448 and 640 cm^{-1} which were assigned to the rutile phase. This indicates that the conversion of anatase to rutile was almost 100 %. The extent of conversion of anatase to rutile through thermal treatment in a furnace following laser irradiation clearly depends on the laser irradiation time prior to the conventional heating.

4. Conclusion

Raman and anti stokes Raman spectroscopy has characterised the effect of exposure to high power laser radiation on the crystalline phases of TiO_2. Raman and anti-stokes Raman provided information on both the structural changes and the kinetics of the crystalline phase change. Measurement of the changes over several time integrals in the Raman and anti-stokes Raman spectra of TiO_2, with exposure to laser radiation, showed that the anatase phase of TiO_2 was converted to the rutile phase. The effects of laser exposure created increasing amounts of rutile from anatase during exposure to laser irradiation. Raman and anti-stokes Raman spectra displayed bands at 144 (A_{1g}), 197 (E_g), 398 (B_{1g}), 515 (A_{1g}), and 640 (E_g) cm^{-1} which were assigned to anatase which are replaced by bands at 143 (B_{1g}), 235 (2 phonon process), 448 (E_g) and 612 (A_{1g}) cm^{-1} which are assigned to rutile. The results of this study demonstrate that Raman spectroscopy is an effective technique for monitoring the laser modification of the crystal structure of TiO_2 materials. This method could be used as an in-situ monitoring technique while the laser modification process is in operation. This would enable precise control of the ratio of the anatase and rutile phases in TiO_2 photocatalyst materials, which has not been possible to date using conventional thermal processing methods.

References.

1. A.L Linsebigler, G. Lu, J.T. Yates, Chem. Rev. 95, (1995) 735.
2. A. Mills, S. Le Hunte, J. Photochem. Photobiol. A: Chem 108 (1997) 1..
3. M.R. Hoffmann, S.T. Martin, W. Choi, D.W. Bahnemann, Chem. Rev. 95 (1995) 69
4. J.L. Ferry, W.H. Glaze, Langmuir, 14 (1998) 3551
5. B. O'Reagan, M. Gratzel, Nature, 353 (1991) 737
6. T.E. Mallouck, Nature, 353 (1998) 698.
7. A. Sclafani, J.M. Herrmann, J. Phys. Chem. 100 (1996) 13655
8. A. Mills, S.J. Morris, S. J. Photochem. Photobio A: Chem. 71 (1993) 75.
9. H.P. Maruska, A.K. Ghosh, Solar Energy, 20 (1978) 443.
10. U. Balachandran, N.G. Eror, J. Solid State Chem. 42 (1982) 276
11. R.S. Katiyar, R.S. Krishnan, Phys. Lett., 25A (1967) 525
12. H. Berger, H.. Tang, F.J. Levy, Crystal Growth, 130 (1993) 108.
13. M. Gotic, S. Popovic, S. Music, A. Selulic, A. Tukovic, K.J. Furic, J. Raman Spec., 28 (1997) 555.
14. G.A. Tompsett, G.A. Bowmaker, B.P. Cooney, J.B. Metson, K.A. Rodgers, J. Raman Spec. 26 (1995) 57.
15. A. Chaves, K.S. Katiyan, S.P.S Porto, Phys. Rev., 10 (1974) 3522.
16. A. Turkovic, M. Ivanda, V. Drasner, V. Vranesa, M. Persin, Thin Solid Films, 198 (1997) 199.
17. S-K Lee, P.K.J. Robertson, A. Mills, D. McStay, J. Photochem, Photobiol., A, Chem., 122, (1999) 69.

18. S-K Lee, P.K.J. Robertson, D. McStay, A. Mills, N. Elliot, D. McPhail, Appl. Catal. B: Environ., 44 (2003) 173.
19. G. Vrillet, S-K Lee, D. McStay, P.K.J. Robertson, Appl. Surf. Sci., 222 (2004) 33
20. T. Ohsaka, F. Izumi, Y. Fujiki, J. Raman Spect. 7 (1978) 321.

Legends for Figures.

Fig. 1. Schematic diagram of the Raman system.

Fig. 2. Raman spectra of TiO_2. λ_{ex} 514 nm, energy at sample 100 mW at sample. (a) initial sample, (b) irradiation for 10 min, (c) a-b.

Fig. 3. Anti-stokes spectra of TiO_2. λ_{ex} 514 nm, energy at sample 100 mW (a) initial sample, (b) irradiation for 10 min, (c) a-b.

Fig. 4. Raman spectra of TiO_2, λ_{ex} 514 nm, energy at sample 100 mW. (a) Initial sample, (b) irradiation for 2 min. (c) irradiation for 4 min., (d) irradiation for 6 min., (e) irradiation for 8 min. and (f) irradiation for 10 min.

Fig. 5. Anti-stokes spectra of TiO_2. λ_{ex} 514 nm, energy at sample 100 mW. (a) initial sample, (b) irradiation for 2 min. (c) irradiation for 4 min., (d) irradiation for 6 min., (e) irradiation for 8 min., and (f) irradiation for 10 min.

Fig. 6. Graph showing irradiation time vs signal height for bands centred at 236 and 515 cm^{-1} observed in Figure 4.

Fig. 7. Raman spectra of TiO_2. λ_{ex} 514 nm, energy at sample 100 mW. (a) TiO_2 irradiated for four min. (b) Sample a) heated at 500 ^oC for 30 min. (c) TiO_2 irradiated for 10 min (d) sample c) heated at 500 ^oC for 30 min.

Table 1. Comparisons of positions (cm^{-1}) of the vibrational modes of TiO_2. (vs=very strong, S=strong, m=medium, w=weak, sh=shoulder band, c=combination.)

Fig. 1.

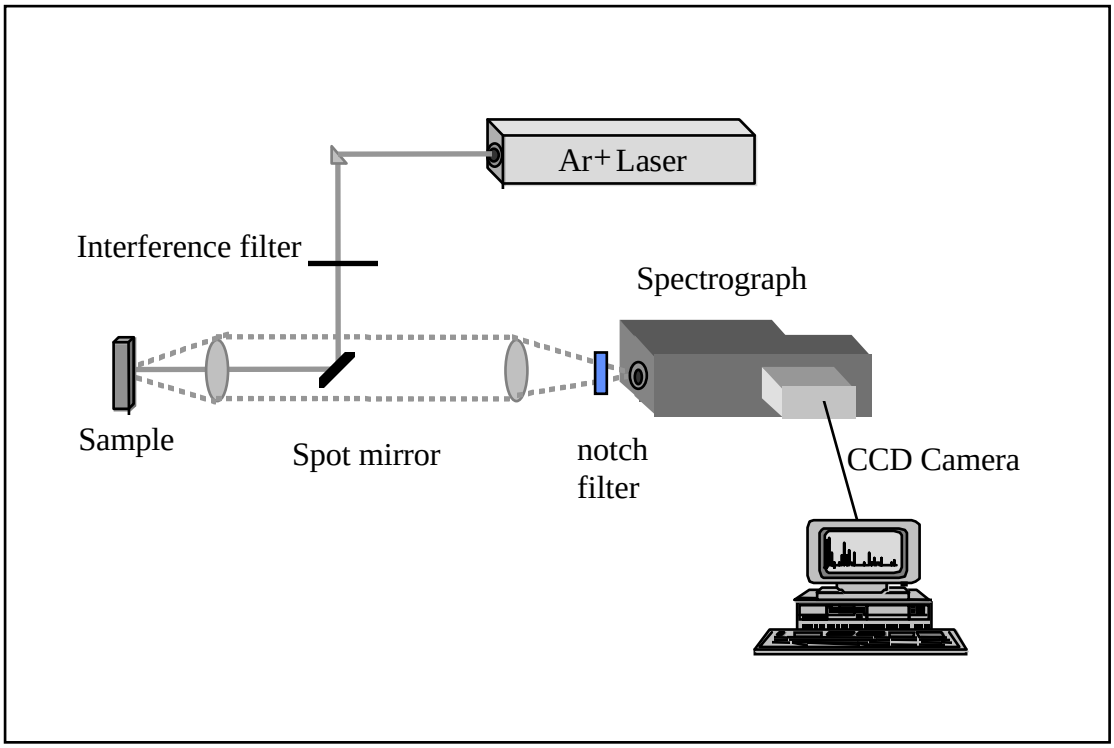
Ar+ Laser
Interference filter
Spectrograph
Sample
Spot mirror
notch
filter
CCD Camera

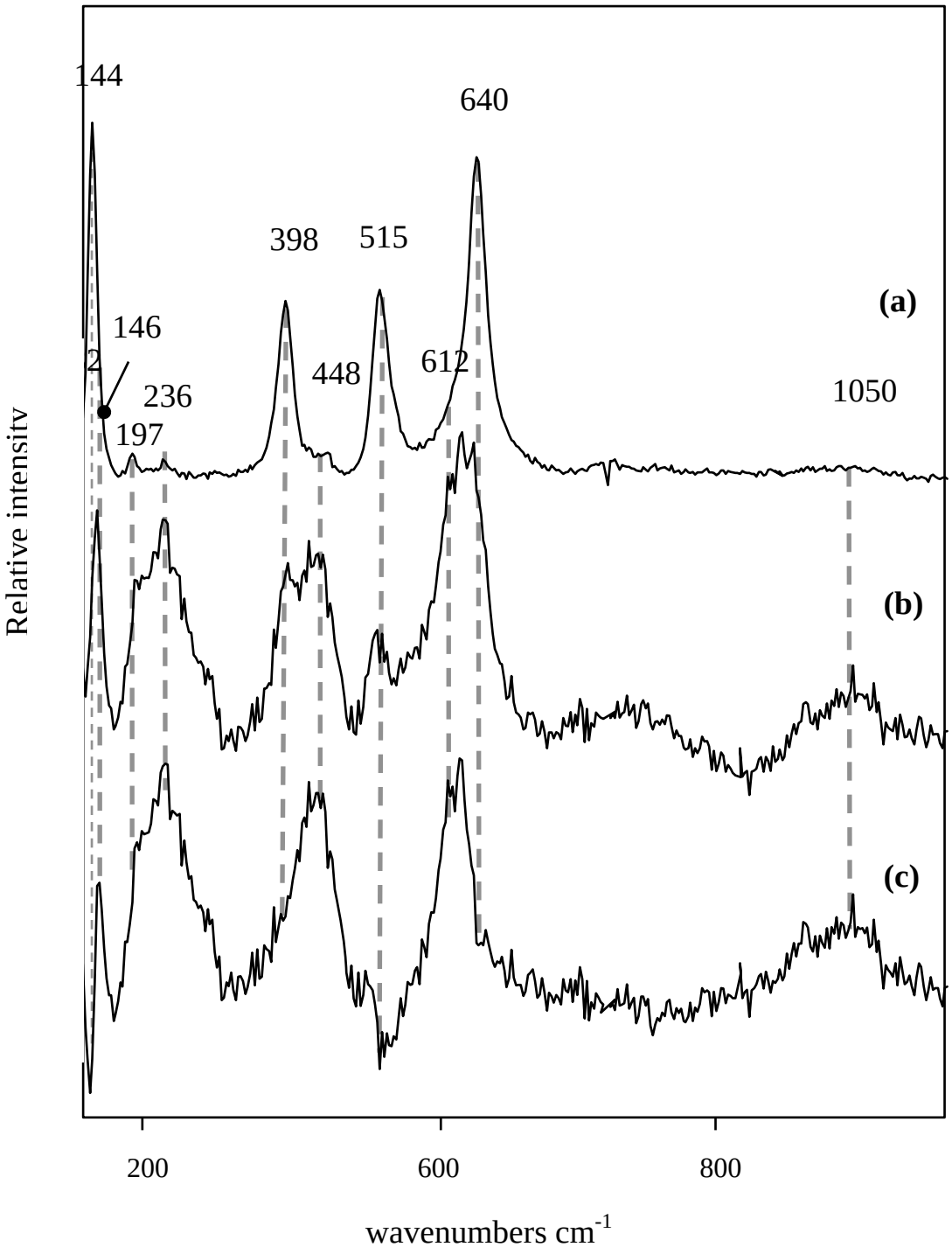
144
640
398
515
146
2
448
612
236
1050
197
(a)
(b)
(c)
Relative intensity
200
600
800
wavenumbers cm-1

Fig. 2.

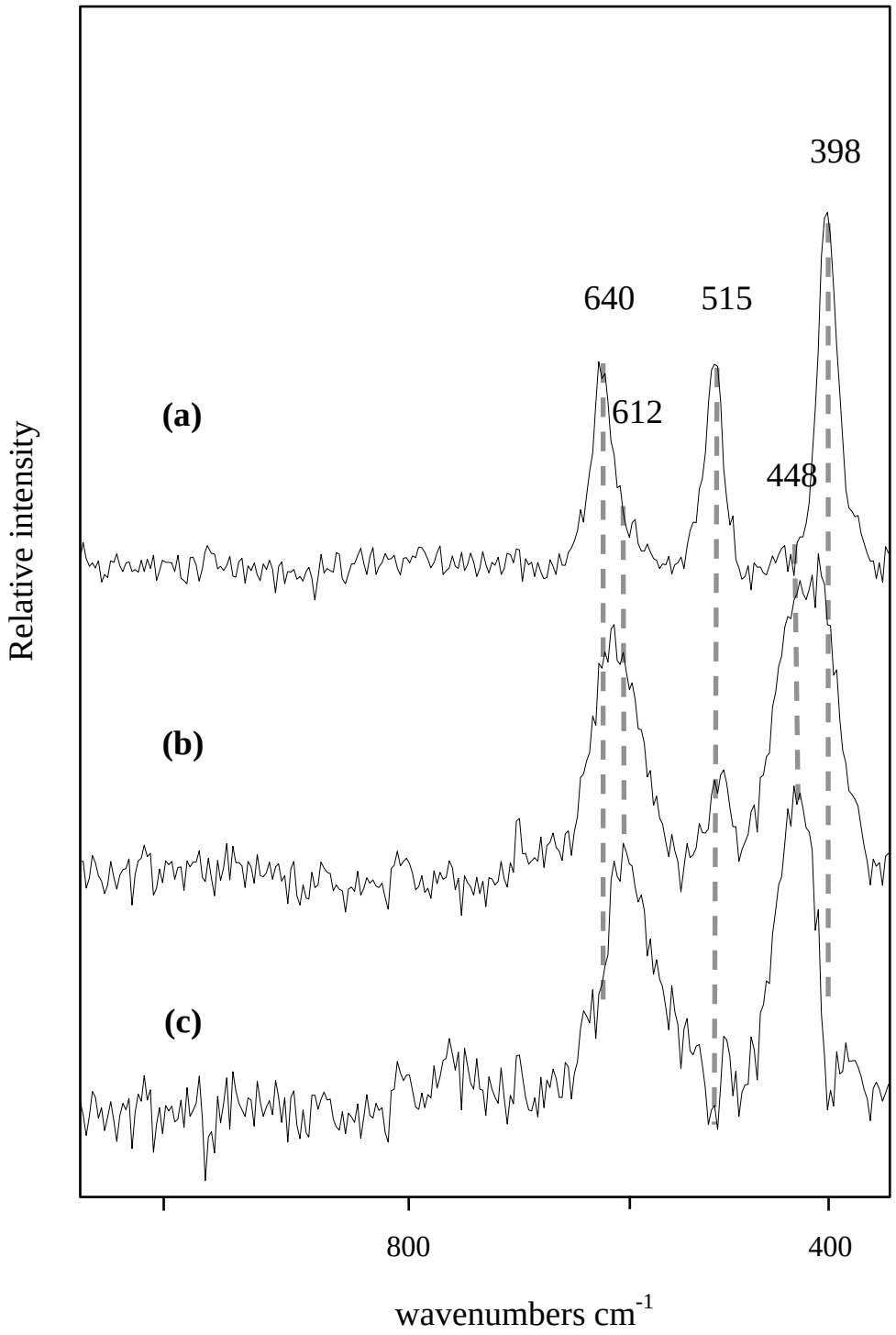
398
640
515
612
448
(a)
(b)
(c)
Relative intensity
800
400
wavenumbers cm-1

Fig. 3.

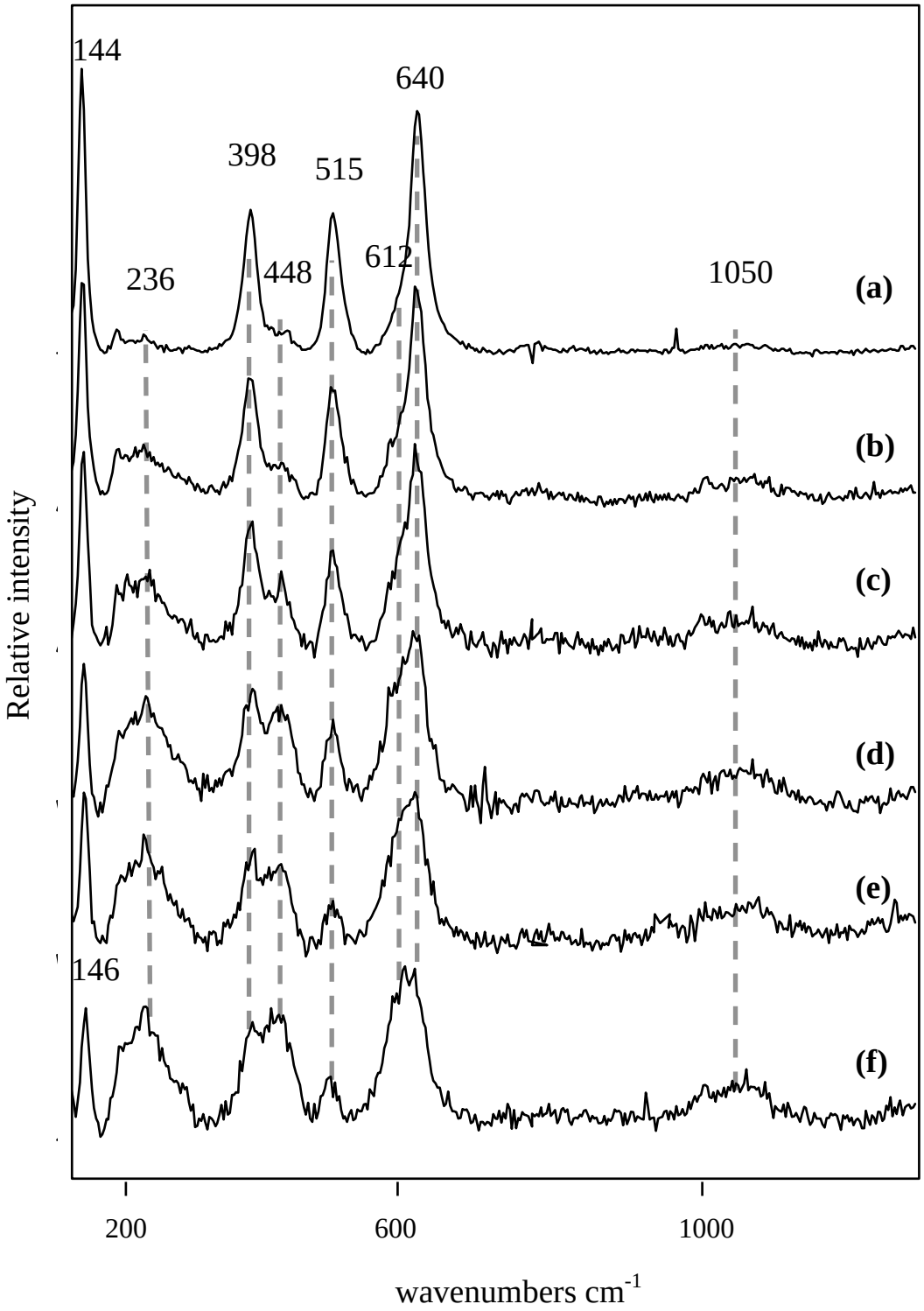
144
640
398
515
612
236
448
1050
(a)
(b)
(c)
(d)
(e)
146
(f)
Relative intensity
200
600
1000
wavenumbers cm-1

Fig. 4.

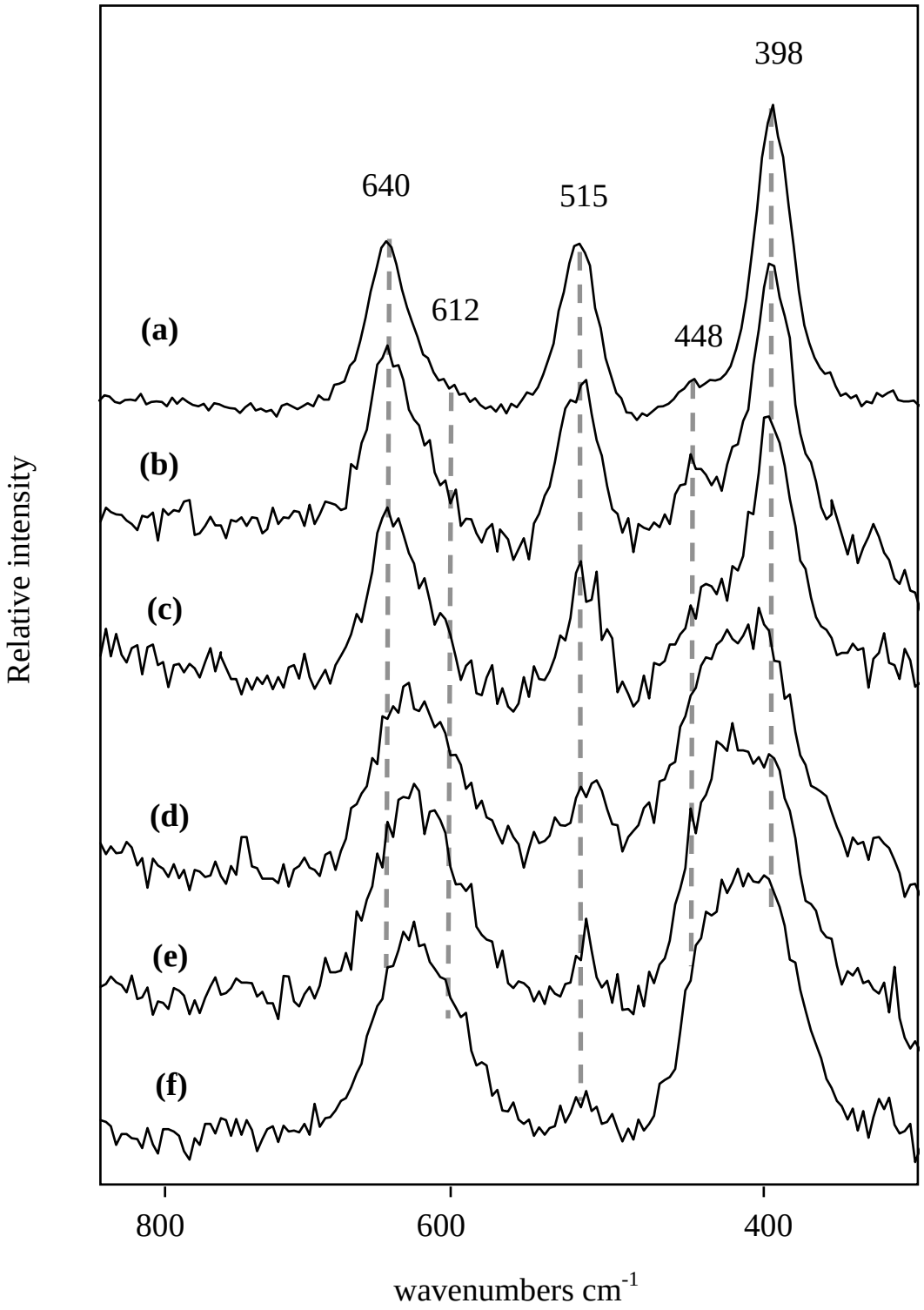
398
640
515
612
448
(a)
(b)
(c)
(d)
(e)
(f)
Relative intensity
800
600
400
wavenumbers cm-1

Fig. 5.

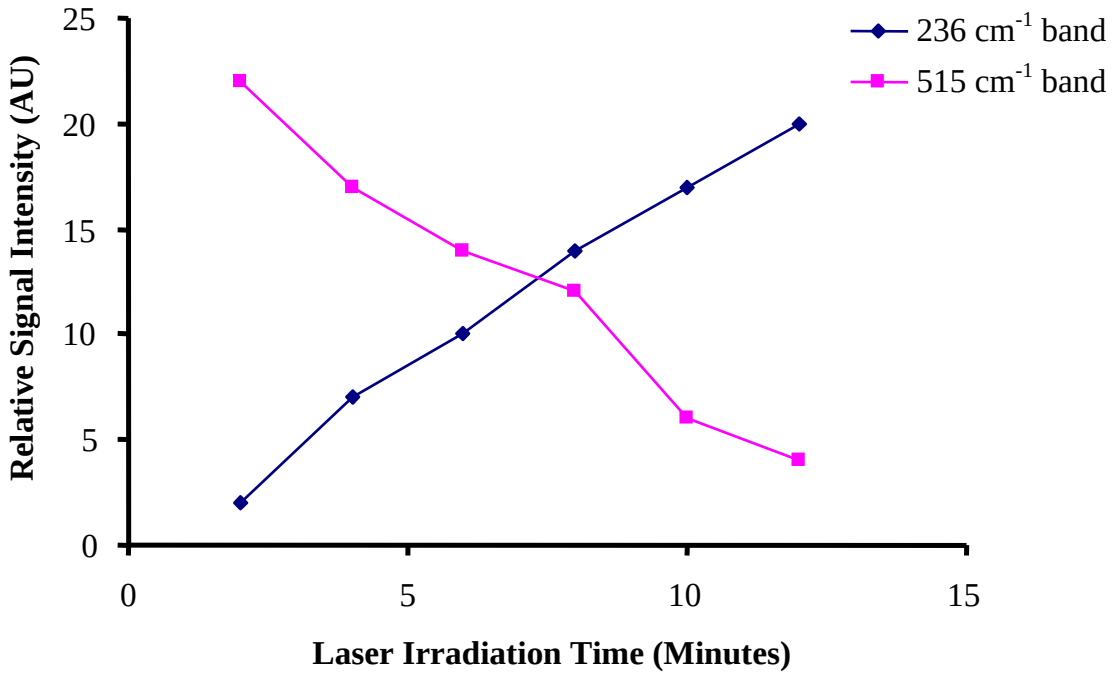
Relative Signal Intensity (AU)
25
20
15
10
5
0
0
5
10
15
Laser Irradiation Time (Minutes)
236 cm-1 band
515 cm-1 band

Fig. 6

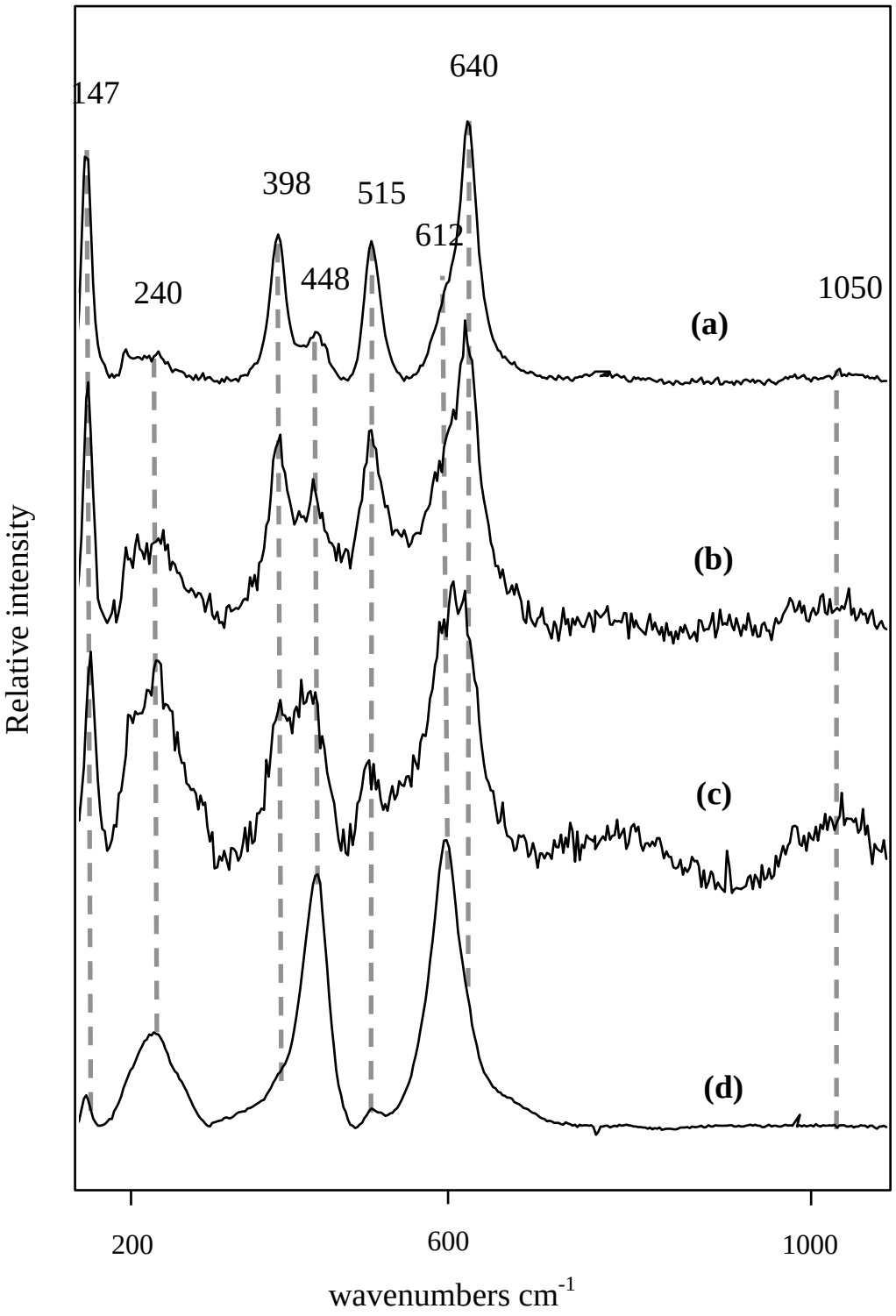
147
640
398
515
612
448
240
1050
(a)
(b)
(c)
(d)
Relative intensity
200
600
1000
wavenumbers cm-1

Fig. 7

Brookite [11]	**Anatase [11]**	**Rutile [11]**	**Degussa P25 (80% Anatase:20% rutile)**	**P25 Sample Laser Irradiated for 10 Mins**
128 (s) 135 (w)				
	144 (vs) Eg	143 (w) B1g	144 (vs)	144(vs) 146(w)
153 (vs) 172 (sh)				
195 (w)	197 (w) Eg		197 (w) Eg	
214 (w)				
		235 (m) *c*	236 (w) *c*	236 (s)
247 (m)				
		273 (sh)		
288 (w)				
322 (w)	320 (vs) *c*	320 (w)		
366 (w)		357 (w)		
396 (sh)	399 (s) B1g		398 (s)	398 (s)
412 (w)				
454 (w)		447 (s) Eg	448 (w)	448 (s)
461 (w)				
502 (w)				
	515 (m) A1g		515 (s)	515 (s)
	519 (m) B1g			
545 (w)				
585 (w)				
		612 (s) A1g	612 (w)	612 (s)
636 (s)	639 (m) Eg		640 (s)	640 (s)
	795 (w) B1g			
	over	826 (w) B2g		
				1050 (w)

Table 1.